Structure Factors for Hot Neutron Matter from *Ab Initio* Lattice Simulations with High-Fidelity Chiral Interactions

Yuan-Zhuo Ma,[1,2] Zidu Lin,[3] Bing-Nan Lu,[4] Serdar Elhatisari,[5,6] Dean Lee,[2,*] Ning Li,[7] Ulf-G. Meißner,[6,8,9] Andrew W. Steiner,[3,10] and Qian Wang[1]

[1]*Key Laboratory of Atomic and Subatomic Structure and Quantum Control (MOE), Guangdong Basic Research Center of Excellence for Structure and Fundamental Interactions of Matter, Institute of Quantum Matter, South China Normal University, Guangzhou 510006, China*

[2]*Facility for Rare Isotope Beams and Department of Physics and Astronomy, Michigan State University, Michigan 48824, USA*

[3]*Department of Physics and Astronomy, University of Tennessee, Knoxville, Tennessee, USA*

[4]*Graduate School of China Academy of Engineering Physics, Beijing 100193, China*

[5]*Faculty of Natural Sciences and Engineering, Gaziantep Islam Science and Technology University, Gaziantep 27010, Turkey*

[6]*Helmholtz-Institut für Strahlen- und Kernphysik and Bethe Center for Theoretical Physics, Universität Bonn, D-53115 Bonn, Germany*

[7]*School of Physics, Sun Yat-Sen University, Guangzhou 510275, China*

[8]*Institute for Advanced Simulation, Institut für Kernphysik, and Jülich Center for Hadron Physics, Forschungszentrum Jülich, D-52425 Jülich, Germany*

[9]*Tbilisi State University, 0186 Tbilisi, Georgia*

[10]*Physics Division, Oak Ridge National Laboratory, Oak Ridge, Tennessee, USA*

(Received 13 June 2023; revised 27 February 2024; accepted 8 May 2024; published 5 June 2024)

We present the first *ab initio* lattice calculations of spin and density correlations in hot neutron matter using high-fidelity interactions at next-to-next-to-next-to-leading order in chiral effective field theory. These correlations have a large impact on neutrino heating and shock revival in core-collapse supernovae and are encapsulated in functions called structure factors. Unfortunately, calculations of structure factors using high-fidelity chiral interactions were well out of reach using existing computational methods. In this Letter, we solve the problem using a computational approach called the rank-one operator (RO) method. The RO method is a general technique with broad applications to simulations of fermionic many-body systems. It solves the problem of exponential scaling of computational effort when using perturbation theory for higher-body operators and higher-order corrections. Using the RO method, we compute the vector and axial static structure factors for hot neutron matter as a function of temperature and density. The *ab initio* lattice results are in good agreement with virial expansion calculations at low densities but are more reliable at higher densities. Random phase approximation codes used to estimate neutrino opacity in core-collapse supernovae simulations can now be calibrated with *ab initio* lattice calculations.

DOI: 10.1103/PhysRevLett.132.232502

Introduction.—Core-collapse supernovae (CCSNe) are catastrophic events heralding the death of massive stars. Under enormous gravitational pressure, the nickel-iron core converts to neutron-rich matter via inverse beta decay. This results in an infall of stellar matter followed by a violent rebound from the ultradense core. Meanwhile, copious numbers of neutrinos are produced. This neutrino flux provides energy to the shock wave and increases the likelihood of an explosion. Since the neutrino-nucleon scattering rates are greatly modified by the spin and density correlations in neutron-rich matter, understanding these correlations is important for modeling CCSNe explosions [1–4]. Early efforts in studying in-medium neutrino-nucleon scattering have used mean field methods such as the Hartree-Fock and random phase approximations (RPA) [5–8]. Extended virial expansions provide model-independent predictions in the limit of low densities and high temperatures [7–11].

More recently, *ab initio* lattice calculations of neutron matter and its structure factors were performed using pionless effective field theory at leading order, both in the limit of infinite scattering length [12] and at the physical scattering length [13]. These calculations are suitable for environments where the neutrons have momenta less than 100 MeV. We are using natural units where the speed of light, c, reduced Planck constant, $\hbar$, and Boltzmann constant, k_B, are set to unity. In order to describe neutron matter at densities and temperatures relevant for CCSNe, a good description of nucleons up to 300 MeV momenta is needed. The standard theoretical framework for this regime is provided by chiral effective field theory, where the forces mediated by the exchange of pions are treated explicitly [14,15].

Recent advances in chiral effective field theory interactions and advanced quantum many-body methods have pushed forward the frontiers of *ab initio* nuclear

calculations. Calculations are now possible for light nuclei [16–21], medium-mass [22–26] and heavy nuclei [27], and nuclear matter [28–31], as well as finite temperature systems [32–37]. In this Letter, we compute the spin and density correlations in neutron matter at various temperatures and densities using lattice chiral effective field theory at next-to-next-to-next-to leading order (N3LO). Such N3LO lattice calculations were previously not possible due to the many perturbation theory corrections required and the lack of a practical method for computing the corrections efficiently.

In this Letter, we introduce a new computational approach called the rank-one operator (RO) method. In many-body theory, rank-one operators are one-body operators where one creation operator multiplies one annihilation operator. As we will show, rank-one operators are special since they can be inserted into auxiliary-field Monte Carlo calculations without the need to compute derivatives with respect to parameters. The RO method uses this property of rank-one operators to solve the problem of exponential scaling of computational effort when using perturbation theory for higher-body operators and higher-order corrections. It can be used with Monte Carlo calculations of fermionic systems in nuclear physics, condensed matter, ultracold atomic gases, and quantum chemistry.

Methods.—Nuclear lattice effective theory (NLEFT) is an *ab initio* method that combines effective field theory with lattice Monte Carlo simulations [16,23,35,38–44]. The use of unrestricted Monte Carlo simulations allows for investigations of strong many-body correlations such as clustering [43,45,46]. Moreover, the pinhole trace algorithm [35] allows for *ab initio* calculations of nuclear thermodynamics.

For fixed neutron number N and temperature T, the expectation value of an observable O in the canonical ensemble (CE) is given by

$$\langle O\rangle_N = \frac{Z_{\mathcal{O}}(\beta,N)}{Z(\beta,N)} = \frac{\mathrm{Tr}_N(e^{-\beta H}O)}{\mathrm{Tr}_N(e^{-\beta H})}, \tag{1}$$

where $\beta = T^{-1}$ is the inverse of temperature, H is the Hamiltonian, and Tr_N is the trace over all the N-neutron states. The canonical partition function $Z(\beta,N)$, can be written explicitly in the single-particle basis $c_i = (\boldsymbol{n}_i, \sigma_i, \tau_i)$ as

$$Z(\beta,N) = \sum_{c_1,\ldots,c_N} \langle c_1,\ldots,c_N|\exp(-\beta H)|c_1,\ldots,c_N\rangle, \tag{2}$$

with $\boldsymbol{n}_i$ an integer triplet specifying the lattice coordinates, σ_i is the spin, and $\tau_i = -1/2$ is the isospin for neutrons. To update and sum over initial and final states we implement the pinhole trace algorithm described in Ref. [35].

We break up the exponential $\exp(-\beta H)$ as a product of transfer matrices, which are just short-time exponentials for each lattice time step. In the auxiliary-field formalism, the transfer matrices depend on the auxiliary fields and pion fields [16,39]. The transfer matrix $M(n_t)$ corresponds to time step n_t. If we use L_t total time steps, then we get a product of the form $M(L_t-1)\cdots M(0)$. We use the shuttle algorithm described in Ref. [23] to update the auxiliary fields and pion fields.

It is also convenient to consider the partition function for the grand canonical ensemble (GCE),

$$\mathcal{Z}(\beta,\mu_G) = \sum_N e^{\beta\mu_G N} Z(\beta,N), \tag{3}$$

where μ_G is chemical potential. The expectation of an operator in the GCE can be evaluated as

$$\langle O\rangle_G = \frac{\sum_N \langle O\rangle_N e^{\beta\mu_G N} Z(\beta,N)}{\sum_N e^{\beta\mu_G N} Z(\beta,N)} = \sum_N \langle O\rangle_N w_N, \tag{4}$$

where w_N is the normalized neutron number probability. This distribution function w_N can be obtained by calculating CE partition function $Z(\beta,N) = e^{-\beta F(\beta,N)}$, where the free energy $F(\beta,N)$ is the integration of the CE chemical potential $\mu(\beta,n)$ from an N_0-particle system, $F(\beta,N) = F(\beta,N_0) + \int_{N_0}^{N} \mu(\beta,n)dn$. We use the Widom insertion method [35,47,48] to calculate the CE chemical potential $\mu(\beta,n)$. Further details are presented in the Supplemental Material [49].

A primary challenge for NLEFT calculations is the Monte Carlo sign problem, caused by cancellations between positive and negative amplitudes. In order to mitigate this problem, we start from a simple interaction with no significant sign oscillations and use the perturbation theory to implement the difference between the simple interaction and the high-fidelity interaction. Perturbative calculations up to the second order correction in the energy have been implemented in lattice quantum Monte Carlo simulations [44]. In this work we perform the first order perturbation to bridge the gap between simple and high-fidelity chiral interactions. However, we greatly accelerate the convergence of perturbation theory using high-fidelity interactions generated using the method of wave function matching as described in Ref. [56].

In the auxiliary-field formalism, we work with Slater determinant wave functions and transfer matrices $M(n_t)$ that consist of exponentials of one-body operators that are normal ordered so that annihilation operators are on the right and creation operators are on the left. As a result, the many-body amplitude equals the matrix determinant of the single-nucleon amplitudes. At zeroth order in perturbation theory, we simply replace each $M(n_t)$ by the unperturbed transfer matrix $M^{(0)}(n_t)$. In order to calculate perturbation theory corrections, we introduce additional terms into the transfer matrices,

$$M(n_t) = M^{(0)}(n_t) + \sum_\theta t_\theta(n_t) O_\theta \cdots, \tag{5}$$

where each O_θ is a normal-ordered one-body operator. We can insert the operator O_θ wherever desired by taking the derivative with respect to the corresponding parameter $t_\theta(n_t)$ and setting all such parameters to zero thereafter. In this manner, we can build higher-body operators from products of the one-body operators O_θ and compute corrections to any order in perturbation theory.

Unfortunately, the severe computational challenge one faces is that taking k such derivatives requires $O(2^k)$ terms. The exponential scaling is readily seen when one calculates the derivatives using finite differences. Each finite difference requires a forward and backward step, and this produces 2^k terms for k derivatives. The Jacobi formulas for derivatives of matrix determinants [39] allows us to calculate the derivatives exactly without finite differences; however, the scaling of computational effort is still $O(2^k)$.

The RO method avoids this exponential scaling by using one-body operators O_θ that have the form $F^\dagger_{\alpha'}F_\alpha$, where F_α is the annihilation operator for nucleon orbital α and $F^\dagger_{\alpha'}$ is the creation operator for nucleon orbital α'. Since F_α can only annihilate one nucleon and $F^\dagger_{\alpha'}$ can only create one nucleon, it is a rank-one operator. We conclude that the amplitude has no terms that contain more than one power of the coefficient $t_\theta(n_t)$. Instead of inserting O_θ by taking the derivative with respect to $t_\theta(n_t)$, we can simply take $t_\theta(n_t)$ to be very large and divide the amplitude by $t_\theta(n_t)$. Since this requires the calculation of one amplitude rather than two amplitudes, the problem of exponential scaling is solved.

Static structure factors are Fourier transforms of the fluctuations of the spin and density correlation functions. Let $\hat{\rho}$ and $\hat{\rho}_z$ be the particle density and spin density operators, respectively. Let ρ^0 be the average particle density and ρ_z^0 be the average spin density. Here, we consider unpolarized neutron matter where ρ_z^0 equals zero. On the lattice, the vector and axial static structure factors can be written as

$$S_{\rm v}(\boldsymbol{q}) = \frac{1}{L^3}\sum_{\boldsymbol{n}\boldsymbol{n}'} e^{-i\boldsymbol{q}\cdot\boldsymbol{n}}[\langle\hat{\rho}(\boldsymbol{n}+\boldsymbol{n}')\hat{\rho}(\boldsymbol{n}')\rangle - (\rho^0)^2],$$
$$S_{\rm a}(\boldsymbol{q}) = \frac{1}{L^3}\sum_{\boldsymbol{n}\boldsymbol{n}'} e^{-i\boldsymbol{q}\cdot\boldsymbol{n}}[\langle\hat{\rho}_z(\boldsymbol{n}+\boldsymbol{n}')\hat{\rho}_z(\boldsymbol{n}')\rangle - (\rho_z^0)^2], \quad (6)$$

where $\boldsymbol{n}, \boldsymbol{n}'$ represents coordinate on a L^3 cubic lattice. The expectation values of these two-body density correlation operators in Eq. (6) are calculated using the RO formalism. Further details can be found in the Supplemental Material [49].

Results.—We perform simulations on $L^3 = 6^3, 7^3, 8^3$ cubic lattices with spatial lattice spacing $a = 1/(150\ \text{MeV}) \approx 1.32$ fm and temporal lattice spacing $a_t = 1/(1000\ \text{MeV})$. Following the strategy in Ref. [35], we use twist-averaged boundary conditions to eliminate finite volume effects and accelerate the convergence to the thermodynamic limit. For twist angle θ_i along each spatial direction i, the possible lattice momenta are $2\pi n_i/L + \theta_i/L$, with some integer n_i. The averaging over all possible twist angles θ_i is done by Monte Carlo sampling.

In Fig. 1 we present NLEFT results in the GCE for the static structure factors $S_{\rm v}$ and $S_{\rm a}$ in the long wavelength limit, $q \to 0$. The results are calculated at a temperature of 20 MeV and plotted as a function of density. We show lattice results corresponding to the high-fidelity N3LO chiral interaction generated using wave function matching (WFM) [56]. For comparison, we show results obtained with RPA calculations using NRAPR [57], SGII [58], SVmin [59], and UNEDF [60] Skyrme interactions. We also show several virial expansion calculations, which we now discuss.

The virial expansion is an expansion in powers of the fugacity $z = \exp(\mu/T)$. We also make use of an approximate idealization of pure neutron matter called the unitary limit, where the interaction range is zero and the scattering length is infinite. The results labeled as Virial2 in Fig. 1

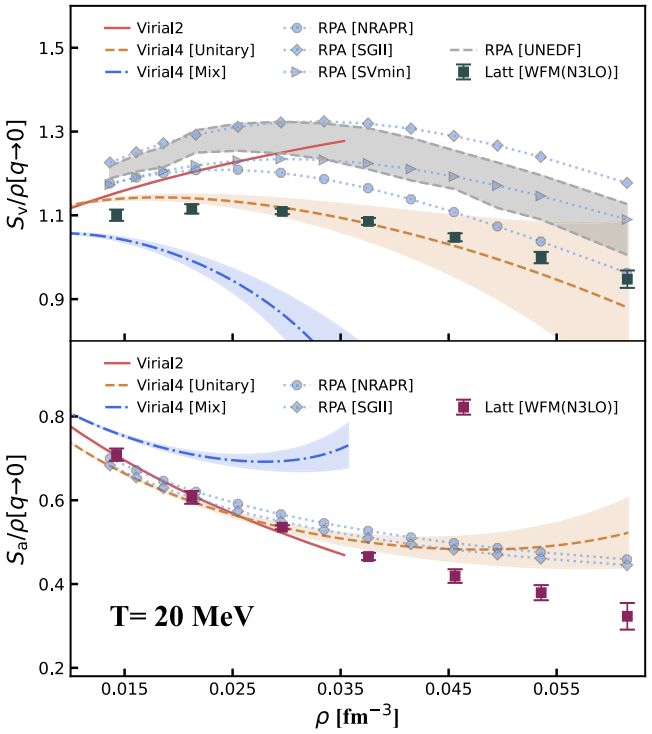

FIG. 1. Calculated static structure factors of $S_{\rm v}$ and $S_{\rm a}$ at the long-wavelength limit ($q \to 0$) with $T = 20$ MeV. Virial2 denotes second order virial calculations using physical neutron data. Virial4 [Unitary] corresponds to fourth virial calculations for the unitary limit. Virial4 [Mix] is a hybrid of the two, with the second order term for physical neutrons and the third and fourth order terms for the unitary limit. The RPA calculations are carried out with four different interactions (NRAPR, SGII, SVmin and UNEDF). WFM(N3LO) represents the NLEFT calculations with the wave function matching N3LO interaction.

corresponds to the virial expansion at second order, using physically observed data for the interactions between neutrons [8]. The Virial4 [Unitary] results show virial expansions for the unitary Fermi gas results at fourth order [9]. Higher-order virial coefficients corresponding to physical neutrons are not currently available. The Virial4 [Mix] results corresponds to a hybrid virial calculation where the second order terms correspond to physical neutrons but the third and the fourth order terms are associated with the unitary limit. The error bands on the Virial4 results are associated with uncertainties in the fourth order virial coefficient in the unitary limit. The significant difference between Virial4 [Unitary] and Virial4 [Mix] shows that even a minor change to the interaction has a significant effect on the vector and axial static structure factors.

In the very low-density region, the lattice results are in agreement with both Virial2 and Virial4 [Mix]. For larger densities, the wide difference between Virial2 and Virial4 [Mix] shows that the order-by-order convergence of the virial expansion is slow. Further details are discussed in the Supplemental Material. The Virial4 [Unitary] results intersect with the lattice results near density 0.030 fm^{-3}. However, the deviations with the lattice results can be as large as ∼25% at $n \approx 0.053$ fm^{-3} and ∼5% at $n \approx 0.015$ fm^{-3} for S_a.

The RPA calculations provide self-consistent yet model-dependent calculations of structure factors not only for pure neutron matter but also for beta-equilibrium matter in a wide range of densities and temperatures [61]. The UNEDF interaction has quantified uncertainties of the Skyrme interactions, and we generate an error band of RPA S_v corresponding to these uncertainties. In the axial current channel, we present RPA calculations for NRAPR and SGII, interactions for which the problem of Skyrme interaction spin instabilities do not appear for densities lower than the saturation density of nuclear matter. In both the vector and axial current channels, we note that the structure factors for some of the RPA calculations are in reasonable agreement with the lattice calculations. In the Supplemental Material, we use the lattice results to calibrate the Skyrme interactions used in the RPA calculations and make predictions for the neutrino inverse mean free path. Several corresponding results for the chemical potential, fugacity, density, and pressure are listed in Table I. The uncertainties shown in the graphs and the table are stochastic errors only. We discuss systematic errors at the end of this section.

TABLE I. Calculated grand canonical ensemble fugacity z, density ρ [fm^{-3}], pressure p [MeV/fm^3] with different chemical potential μ [MeV] at $T = 20$ MeV.

μ	−23.78	−16.58	−10.787	−6.450	−2.828
z	0.3045	0.4365	0.5831	0.7243	0.8682
$\rho \times 100$	1.4274(4)	2.122(1)	2.961(1)	3.758(1)	4.560(1)
p	0.2458(1)	0.3618(1)	0.4901(1)	0.6287(1)	0.7737(2)

In Fig. 2, we present the momentum-dependent structure factor calculations at a temperature of 10 MeV in the GCE at density $\rho_G = 0.018$ fm^{-3}. The lattice cutoff momentum is $\pi/a = 470$ MeV, and so the lattice results are most reliable for momenta smaller than this momentum scale. Nevertheless, the lattice results show the expected high-momentum behavior. Both S_v and S_a should equal the system density at large momenta, $S_v(q \to \infty) = S_a(q \to \infty) = \rho$.

At long wavelengths, S_v and S_a have opposite trends. We also present the calculated chemical potentials of 20 CE systems in the inset of Fig. 2, which are used to construct this GCE system. The many-body corrections on the neutral current neutrino-nucleon interactions in CCSNe are usually estimated in the long wavelength limit, which is justified since the typical momentum transfer by scattered neutrinos is small compared to the thermal nucleon momentum $\sqrt{6MT}$, where M is the nucleon mass. Note by applying exact dynamic structure factors in the calculation, the neutral current neutrino-nucleon scattering rates have small but noticeable deviations from the ones estimated in long wavelength limit [62]. Our *ab initio* calculations at finite momentum transfer provide benchmarks for the calculation of dynamic structure factors of pure neutron matter at finite temperatures.

In addition to the statistical errors reported for the lattice results, we estimate an overall systematic uncertainty at the 5% level. The largest sources of systematic errors are due to finite system size errors, uncertainties in the nuclear

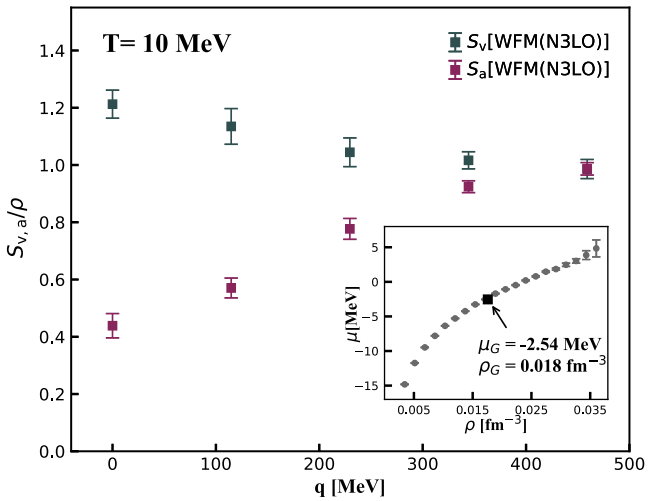

FIG. 2. Calculated momentum-dependent neutron matter structure factors S_v and S_a at $T = 10$ MeV. WFM(N3LO) represents the NLEFT calculations with the wave function matching N3LO interaction. The inset shows calculated chemical potentials of CE systems that are used for the construction of GCE at the chemical potential $\mu_G = -2.54$ MeV and the density $\rho_G = 0.01758(4)$ fm^{-3}.

interaction, and an approximation made in neglecting the numerically small higher-order corrections to the chemical potential, as discussed in the Supplemental Material. The finite system size error was obtained by analyzing the density and pressure with different box sizes. The errors due to uncertainties in the nuclear interaction and the neglected higher-order corrections to the chemical potential were performed by comparing results from calculations at different chiral orders in the canonical ensemble.

Summary.—We have performed the first *ab initio* calculation of structure factors for hot neutron matter using high-fidelity chiral interactions at N3LO. The lattice results of vector and axial structure factors are in good agreement with virial expansions at low densities. The lattice predictions as a function of density, temperature, and momentum transfer provide valuable benchmarks for calibrating RPA and other models commonly used in supernovae simulations. This is detailed in Supplemental Material and further studies are planned in the future.

We have introduced a new computational approach called the rank-one operator method to perform the calculations presented in this work. The rank-one operator method should have immediate applications to Monte Carlo simulations for nearly any quantum many-body systems composed of fermions. With new technologies such as wave function matching available to accelerate the convergence of perturbation theory, one has the possibility of avoiding Monte Carlo sign problems for a large class of fermionic many-body systems. The new computational paradigm requires computing amplitudes with multiple insertions of higher-body operators, and the rank-one operator method is ideally suited for this purpose.

We are grateful for useful discussions with Chuck Horowitz, Gustav Jansen and members of the Nuclear Lattice Effective Field Theory Collaboration. This work has been supported by the Guangdong Major Project of Basic and Applied Basic Research No. 2020B0301030008, the National Natural Science Foundation of China (Grants No. 12105106, No. 12035007 and No. 12275259), China Postdoctoral Science Foundation under Grants No. BX20200136 and No. 2020M682747; Z. L. and A. W. S. were supported by NSF PHY 21-16686. A. W. S. was also supported by the Department of Energy Office of Nuclear Physics. The work of B. N. L. was supported by NSAF No. U2330401. D. L. was supported in part by the U.S. Department of Energy (DE-SC0021152, DE-SC0013365, DE-SC0023658, SciDAC-5 NUCLEI Collaboration). The work of U. G. M. was supported by the European Research Council (ERC) under the European Union's Horizon 2020 research and innovation programme (grant agreement No. 101018170), by Deutsche Forschungsgemeinschaft (DFG, German Research Foundation) (Project-ID 196253076—TRR 110), the Chinese Academy of Sciences (CAS) President's International Fellowship Initiative (PIFI) (Grant No. 2018DM0034), Volkswagen Stiftung (Grant No. 93562) and by the MKW NRW (funding code NW21-024-A). The work of Q. W. was supported by Guangdong Provincial funding with Grant No. 2019QN01X172. Computational resources provided by the Oak Ridge Leadership Computing Facility through the INCITE award "Ab-initio nuclear structure and nuclear reactions," the Southern Nuclear Science Computing Center in the South China Normal University, the Gauss Centre for Supercomputing e.V. [63] for computing time on the GCS Supercomputer JUWELS at the Jülich Supercomputing Centre (JSC), and the Institute for Cyber-Enabled Research at Michigan State University.

*Corresponding author: leed@frib.msu.edu

[1] A. Mezzacappa, Annu. Rev. Nucl. Part. Sci. **55**, 467 (2005).
[2] A. Burrows, S. Reddy, and T. A. Thompson, Nucl. Phys. **A777**, 356 (2006); special Isseu on Nuclear Astrophysics, https://www.sciencedirect.com/science/article/pii/S0375947404007730.
[3] A. Burrows, Rev. Mod. Phys. **85**, 245 (2013).
[4] A. Burrows and D. Vartanyan, Nature (London) **589**, 29 (2021).
[5] R. F. Sawyer, Phys. Rev. C **40**, 865 (1989).
[6] S. Reddy, M. Prakash, J. M. Lattimer, and J. A. Pons, Phys. Rev. C **59**, 2888 (1999).
[7] C. Horowitz and A. Schwenk, Phys. Lett. B **642**, 326 (2006).
[8] C. J. Horowitz, O. L. Caballero, Z. Lin, E. O'Connor, and A. Schwenk, Phys. Rev. C **95**, 025801 (2017).
[9] Z. Lin and C. J. Horowitz, Phys. Rev. C **96**, 055804 (2017).
[10] C. E. Berger, K. J. Morrell, and J. E. Drut, Phys. Rev. A **102**, 023309 (2020).
[11] Y. Hou and J. E. Drut, Phys. Rev. Lett. **125**, 050403 (2020).
[12] A. Alexandru, P. F. Bedaque, and N. C. Warrington, Phys. Rev. C **101**, 045805 (2020).
[13] A. Alexandru, P. Bedaque, E. Berkowitz, and N. C. Warrington, Phys. Rev. Lett. **126**, 132701 (2021).
[14] E. Epelbaum, H.-W. Hammer, and U.-G. Meißner, Rev. Mod. Phys. **81**, 1773 (2009).
[15] R. Machleidt and D. R. Entem, Phys. Rep. **503**, 1 (2011).
[16] D. Lee, Prog. Part. Nucl. Phys. **63**, 117 (2009).
[17] E. Epelbaum, H. Krebs, T. A. Lähde, D. Lee, and U.-G. Meißner, Phys. Rev. Lett. **109**, 252501 (2012).
[18] S. Pastore, A. Baroni, J. Carlson, S. Gandolfi, S. C. Pieper, R. Schiavilla, and R. B. Wiringa, Phys. Rev. C **97**, 022501(R) (2018).
[19] B. R. Barrett, P. Navrátil, and J. P. Vary, Prog. Part. Nucl. Phys. **69**, 131 (2013).
[20] G. Hupin, S. Quaglioni, and P. Navrátil, Nat. Commun. **10**, 351 (2019).
[21] J. Carlson, S. Gandolfi, F. Pederiva, S. C. Pieper, R. Schiavilla, K. E. Schmidt, and R. B. Wiringa, Rev. Mod. Phys. **87**, 1067 (2015).
[22] G. Hagen, T. Papenbrock, M. Hjorth-Jensen, and D. J. Dean, Rep. Prog. Phys. **77**, 096302 (2014).
[23] B.-N. Lu, N. Li, S. Elhatisari, D. Lee, E. Epelbaum, and U.-G. Meißner, Phys. Lett. B **797**, 134863 (2019).

[24] V. Somà, C. Barbieri, T. Duguet, and P. Navrátil, Eur. Phys. J. A **57**, 135 (2021).
[25] R. Wirth, J. M. Yao, and H. Hergert, Phys. Rev. Lett. **127**, 242502 (2021).
[26] S. R. Stroberg, J. D. Holt, A. Schwenk, and J. Simonis, Phys. Rev. Lett. **126**, 022501 (2021).
[27] B. Hu *et al.*, Nat. Phys. **18**, 1196 (2022).
[28] J. E. Lynn, I. Tews, J. Carlson, S. Gandolfi, A. Gezerlis, K. E. Schmidt, and A. Schwenk, Phys. Rev. Lett. **116**, 062501 (2016).
[29] M. Buraczynski and A. Gezerlis, Phys. Rev. Lett. **116**, 152501 (2016).
[30] M. Buraczynski, N. Ismail, and A. Gezerlis, Phys. Rev. Lett. **122**, 152701 (2019).
[31] C. Drischler, J. Holt, and C. Wellenhofer, Annu. Rev. Nucl. Part. Sci. **71**, 403 (2021).
[32] A. Mukherjee and V. R. Pandharipande, Phys. Rev. C **75**, 035802 (2007).
[33] V. Somà and P. Bożek, Phys. Rev. C **80**, 025803 (2009).
[34] A. Carbone and A. Schwenk, Phys. Rev. C **100**, 025805 (2019).
[35] B.-N. Lu, N. Li, S. Elhatisari, D. Lee, J. E. Drut, T. A. Lähde, E. Epelbaum, and U.-G. Meißner, Phys. Rev. Lett. **125**, 192502 (2020).
[36] A. Carbone, Phys. Rev. Res. **2**, 023227 (2020).
[37] J. Keller, K. Hebeler, and A. Schwenk, Phys. Rev. Lett. **130**, 072701 (2023).
[38] D. Lee, Phys. Rev. Lett. **98**, 182501 (2007).
[39] T. A. Lähde and U.-G. Meißner, *Nuclear Lattice Effective Field Theory: An introduction* (Springer, New York, 2019), Vol. 957, ISBN 978-3-030-14187-5, 978-3-030-14189-9.
[40] S. Elhatisari, D. Lee, G. Rupak, E. Epelbaum, H. Krebs, T. A. Lähde, T. Luu, and U.-G. Meißner, Nature (London) **528**, 111 (2015).
[41] S. Elhatisari, N. Li, A. Rokash, J. M. Alarcón, D. Du, N. Klein, B.-n. Lu, U.-G. Meißner, E. Epelbaum, H. Krebs *et al.*, Phys. Rev. Lett. **117**, 132501 (2016).
[42] N. Li, S. Elhatisari, E. Epelbaum, D. Lee, B.-N. Lu, and U.-G. Meißner, Phys. Rev. C **98**, 044002 (2018).
[43] S. Elhatisari, E. Epelbaum, H. Krebs, T. A. Lähde, D. Lee, N. Li, B.-n. Lu, U.-G. Meißner, and G. Rupak, Phys. Rev. Lett. **119**, 222505 (2017).
[44] B.-N. Lu, N. Li, S. Elhatisari, Y.-Z. Ma, D. Lee, and U.-G. Meißner, Phys. Rev. Lett. **128**, 242501 (2022).
[45] N. Summerfield, B.-N. Lu, C. Plumberg, D. Lee, J. Noronha-Hostler, and A. Timmins, Phys. Rev. C **104**, L041901 (2021).
[46] S. Shen, S. Elhatisari, T. A. Lähde, D. Lee, B.-N. Lu, and U.-G. Meißner, Nat. Commun. **14**, 2777 (2023).
[47] B. Widom, The J. Chem. Phys. **39**, 2808 (1963).
[48] K. Binder, Rep. Prog. Phys. **60**, 487 (1997).
[49] See Supplemental Material at http://link.aps.org/supplemental/10.1103/PhysRevLett.132.232502, which includes Refs. [50–55], for additional discussions about the method and results.
[50] P. Reinert, H. Krebs, and E. Epelbaum, Eur. Phys. J. A **54**, 86 (2018).
[51] N. Li, S. Elhatisari, E. Epelbaum, D. Lee, B.-N. Lu, and U.-G. Meißner, Phys. Rev. C **98**, 044002 (2018).
[52] V. G. J. Stoks, R. A. M. Klomp, M. C. M. Rentmeester, and J. J. de Swart, Phys. Rev. C **48**, 792 (1993).
[53] D. Lee, S. Bogner, B. A. Brown, S. Elhatisari, E. Epelbaum, H. Hergert, M. Hjorth-Jensen, H. Krebs, N. Li, B.-N. Lu *et al.*, Phys. Rev. Lett. **127**, 062501 (2021).
[54] T. A. Lähde, T. Luu, D. Lee, U.-G. Meißner, E. Epelbaum, H. Krebs, and G. Rupak, Eur. Phys. J. A **51**, 92 (2015).
[55] E. D. Kuhnle, H. Hu, X.-J. Liu, P. Dyke, M. Mark, P. D. Drummond, P. Hannaford, and C. J. Vale, Phys. Rev. Lett. **105**, 070402 (2010).
[56] S. Elhatisari, L. Bovermann, Y.-Z. Ma, E. Epelbaum, D. Frame, F. Hildenbrand, M. Kim, Y. Kim, H. Krebs, T. A. Lähde, D. Lee *et al.*, Nature (London) (2024), 10.1038/s41586-024-07422-z.
[57] A. W. Steiner, M. Prakash, J. M. Lattimer, and P. J. Ellis, Phys. Rep. **411**, 325 (2005).
[58] N. van Giai and H. Sagawa, Phys. Lett. **106B**, 379 (1981).
[59] P. G. Reinhard and W. Nazarewicz, Phys. Rev. C **81**, 051303(R) (2010).
[60] J. D. McDonnell, N. Schunck, D. Higdon, J. Sarich, S. M. Wild, and W. Nazarewicz, Phys. Rev. Lett. **114**, 122501 (2015).
[61] Z. Lin, A. W. Steiner, and J. Margueron, Phys. Rev. C **107**, 015804 (2023).
[62] P. F. Bedaque, S. Reddy, S. Sen, and N. C. Warrington, Phys. Rev. C **98**, 015802 (2018).
[63] www.gauss-centre.eu.